Cavity Cooling of Internal Molecular Motion

Giovanna Morigi,[1] Pepijn W. H. Pinkse,[2] Markus Kowalewski,[3] and Regina de Vivie-Riedle[3]
[1]*Departament de Fisica, Universitat Autonoma de Barcelona, E-08193 Bellaterra, Spain*
[2]*Max-Planck-Institut für Quantenoptik, Hans-Kopfermannstr. 1, D-85748 Garching, Germany*
[3]*Department of Chemistry, Ludwig-Maximilian-Universität München, Butenandtstr. 11, D-81377 München, Germany*
(Received 19 March 2007; published 13 August 2007)

We predict that it is possible to cool rotational, vibrational, and translational degrees of freedom of molecules by coupling a molecular dipole transition to an optical cavity. The dynamics is numerically simulated for a realistic set of experimental parameters using OH molecules. The results show that the translational motion is cooled to a few μK and the internal state is prepared in one of the two ground states of the two decoupled rotational ladders in a few seconds. Shorter cooling times are expected for molecules with larger polarizability.

DOI: 10.1103/PhysRevLett.99.073001 PACS numbers: 33.80.Ps, 32.80.Lg, 42.50.Pq

The preparation of molecular samples at ultralow temperatures offers exciting perspectives in physics and chemistry [1]. This goal is presently pursued by several groups worldwide with various approaches. Two methods for generating ultracold molecules employ photoassociation and Feshbach resonances, and are efficiently implemented on alkali dimers [1]. Another approach uses buffer gases, to which the molecules thermalize [2]. Its application is limited by the physical properties of atom-molecule collisions at low temperatures. Optical cooling of molecules is an interesting alternative, but, contrary to atoms, its efficiency is severely limited by the multiple scattering channels coupled by spontaneous emission, and may only be feasible for molecules which are confined in external traps for very long times [3]. Elegant laser-cooling proposals, based on optical pumping the rovibrational states [4,5] and excitation pulses tailored with optimal control theory [6,7], exhibit efficiencies which are indeed severely limited by spontaneous decay. In [8,9] it was argued that cooling of the molecular external motion could be achieved by using resonators, by enhancing stimulated photon emission into the cavity mode over spontaneous decay. This mechanism was successfully applied for cooling the motion of atoms [10].

In this Letter we propose a method for optically cooling external as well as the *internal* degrees of freedom of molecules. The method relies on the enhancement of the anti-Stokes Raman transitions through the resonant coupling with the modes of a high-finesse resonator, as sketched in Fig. 1. All relevant anti-Stokes transitions are driven by sequential tuning of the driving laser. At the end of the process the molecule is in the rovibrational ground state and the motion is cooled to the cavity linewidth. We demonstrate the method with *ab initio* based numerical simulations using OH radicals, of which cold ensembles are experimentally produced [11,12].

We now outline the theoretical considerations. We consider a gas of molecules of mass M, prepared in the electronic ground state X, and with dipole transitions $X \to E$. Here, E is a set of electronically excited states, including higher-lying states which may contribute significantly to the total polarizability. We denote the rovibrational states and their corresponding frequencies by $|j, \xi\rangle$ and $\omega_\xi^{(j)}$ $(j = X, A, \ldots)$, while the elements of the dipole moment $\mathbf{d}$ are $\mathcal{D}_{\xi\to\xi''} = \langle A \in E, \xi''|\mathbf{d}|X, \xi\rangle$. These transitions are driven by a far-off resonant laser and interact with an optical resonator as illustrated in Fig. 1(a). In absence of the resonator, spontaneous Raman scattering determines the relevant dynamics of molecule-photon interactions. These processes depend on the center-of-mass momentum $\mathbf{p}$ through the Doppler effect and occur at rate $\Gamma^{(\gamma)}_{\xi\to\xi'}(\mathbf{p}) = \sum_{E,\xi''}\Gamma_{\xi''\to\xi'}\gamma_{E,\xi\to\xi''}(\mathbf{p})$, where $\Gamma_{\xi''\to\xi'}$ the decay rate along the transition $|A, \xi''\rangle \to |X, \xi'\rangle$, and

$$\gamma_{E,\xi\to\xi''}(\mathbf{p}) = \frac{\Omega^2_{L,\xi\to\xi''}}{(\Delta^E_{\xi,\xi''} + \mathbf{k_L}\cdot\mathbf{p}/M)^2 + \Gamma^2_{\xi''}/4}, \qquad (1)$$

with $\Gamma_{\xi''} = \sum_{\xi'}\Gamma_{\xi''\to\xi'}$. Here, $\Omega_{L,\xi\to\xi''} = \mathcal{E}_L(\mathcal{D}_{\xi\to\xi''}\cdot\boldsymbol{\epsilon}_L)/\hbar$ gives the strength of coupling to the laser with electric field amplitude $\mathcal{E}_L$, polarization $\boldsymbol{\epsilon}_L$, frequency ω_L, and wave vector $\mathbf{k_L}$, and $\Delta^E_{\xi,\xi''} = \omega^{(X)}_\xi - \omega^{(E)}_{\xi''} + \omega_L$ denotes the detuning between laser and internal transition.

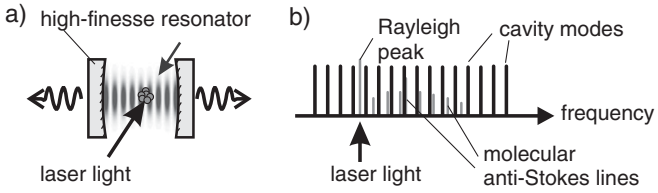

FIG. 1. (a) A molecular sample interacts with the cavity field and is driven by a laser, inducing Raman transitions cooling the internal and external degrees of freedom. (b) Comb of resonances at which photon emission into the cavity is enhanced. The gray bars symbolize the molecular lines, which in OH extend over several tens of nanometers. The laser frequency (arrow) is varied to sequentially address several anti-Stokes lines.

In the limit where the laser is far-off resonant from the electric dipole transitions, electronic ground states at different rovibrational quantum numbers are coupled via Raman transitions. The corresponding emission spectrum is symbolized by the gray bars in Fig. 1(b). In this regime, coupling an optical resonator to the molecule may enhance one or more scattering processes when the corresponding molecular transitions are resonant with resonator modes, symbolized by the black bars in Fig. 1(b). This enhancement requires that the rate $\Gamma^{\kappa}_{\xi\to\xi'}(\mathbf{p})$, describing scattering of a photon from the laser into the cavity mode, and its subsequent loss from the cavity, exceeds the corresponding spontaneous Raman scattering rate, $\Gamma^{\kappa}_{\xi\to\xi'}(\mathbf{p}) \gg \Gamma^{\gamma}_{\xi\to\xi'}(\mathbf{p})$. For a standing wave cavity, in the regime where the molecular kinetic energy exceeds the cavity potential, and when the cavity photon is not reabsorbed but lost via cavity decay [9], we have $\Gamma^{\kappa}_{\xi\to\xi'}(\mathbf{p}) = \Gamma^{\kappa,+}_{\xi\to\xi'}(\mathbf{p}) + \Gamma^{\kappa,-}_{\xi\to\xi'}(\mathbf{p})$, where the sign $\pm$ gives the direction of emission along the cavity axis and

$$\Gamma^{\kappa,\pm}_{\xi\to\xi'}(\mathbf{p}) = 2\kappa \sum_{c,E,\xi''} \frac{\gamma_{E,\xi\to\xi''}(\mathbf{p})|g^{\pm}_{c,\xi''\to\xi'}|^2}{(\delta\omega \pm \mathbf{k_c}\cdot\mathbf{p}/M)^2 + \kappa^2}. \quad (2)$$

Here, 2κ is the cavity linewidth, $\delta\omega = \omega^{(X)}_{\xi} - \omega^{(X)}_{\xi'} + \omega_L - \Omega_c$ is the frequency difference between the initial and final (internal and cavity) state, with Ω_c the frequencies of the cavity modes, and $g^{\pm}_{c,\xi'\to\xi''}$ are the Fourier components at cavity-mode wave vector $\pm|\mathbf{k_c}|$ of the coupling strength to the empty cavity mode, $g_{c,\xi'\to\xi''}(\mathbf{x}) = \mathcal{E}_c(\mathbf{x})(\boldsymbol{\epsilon}_0\cdot\mathcal{D}_{\xi',\xi''})/\hbar$, with $\mathcal{E}_c$ and $\boldsymbol{\epsilon}_0$ the vacuum amplitude and polarization. Note that reabsorption and spontaneous emission of the cavity photon can be neglected while $\kappa \gg |g_{c,\xi'\to\xi''}\Omega_{L,\xi\to\xi''}/\Delta^{E}_{\xi,\xi''}|$.

Enhancement of *Rayleigh* scattering into the cavity is achieved by setting the laser on resonance with one cavity mode, $\omega_L = \Omega_c$, see Fig. 1(b), provided that $\Gamma^{\gamma}_{\xi\to\xi} \ll \Gamma^{\kappa}_{\xi\to\xi}$, i.e., $g^2_{c,\xi\to\xi}/\Gamma\kappa \gg 1$, where Γ is determined by the linewidths of the excited states which significantly contribute to the scattering process. This situation has been discussed in [9], where it has been predicted that the motion can be cavity cooled to a temperature which is in principle only limited by the cavity linewidth [13], provided that the laser is set on the low-frequency side of the cavity resonance. Note that cooling of the motion in the plane orthogonal to the cavity axis is warranted when the laser is a standing wave field, which is simply found in our model by allowing for the absorption of laser photons at wave vector $-\mathbf{k_L}$. In general, enhancement of scattering along the Raman transition $\xi \to \xi'$, decreasing the energy of the rovibrational degrees of freedom, is achieved by setting the laser such that the corresponding anti-Stokes spectral line is resonant with one cavity mode, and requires $g^2_{c,\xi\to\xi'}/\Gamma\kappa \gg 1$. The cooling strategy then consists of choosing a suitable cavity and of sequentially changing the laser frequency, so as to maximize the resonant drive of the different anti-Stokes spectral lines, and thereby cooling the molecule to the rovibrational ground state.

We simulate the cooling dynamics for OH radicals using a rate equation based on the rates (1) and (2). The considered Raman process is detuned from the excitation energy of 32 402 cm^{-1} (971.4 THz) between the $X^2\Pi_i$ ground state and the electronically excited state $A^2\Sigma^+$ as indicated in Fig. 2(b). The relevant rovibrational spectrum and the coupling of the molecule to the laser field and cavity modes were obtained by combining *ab initio* calculations for the vibronic degrees of freedom with available experimental data for the rotational constants. The level scheme is displayed in Fig. 2(b). The potential energy surfaces (PES) and the polarizabilities were calculated with highly correlated quantum chemical methods: the electronic structure calculations [14] were performed on the multiconfigurational self consistent field (MCSCF) level using a single atom basis set (aug-cc-pVTZ). Rates (1) and (2) were evaluated using the polarizability tensors, defined as $\alpha_{\xi\to\xi'} = \sum_{\xi''}\mathcal{D}_{\xi\to\xi''}\mathcal{D}_{\xi''\to\xi'}/\hbar\Delta_{\xi''}$ [15] and calculated with linear response theory at the MCSCF level [16–18]. In order to determine the internal level structure and transition strengths, the vibrational eigenvalues and eigenfunctions were evaluated with a relaxation method using propagation in imaginary time plus an additional diagonalization step [19]. The corresponding Placzek-Teller coefficients [20] were calculated for the transitions between the rotational sublevels.

In order to obtain a concise picture of the cooling dynamics, several assumptions were made without loss of generality. The molecules are prepared in the lower-lying $X^2\Pi_{3/2}$ component of the $X^2\Pi$ electronic ground state.

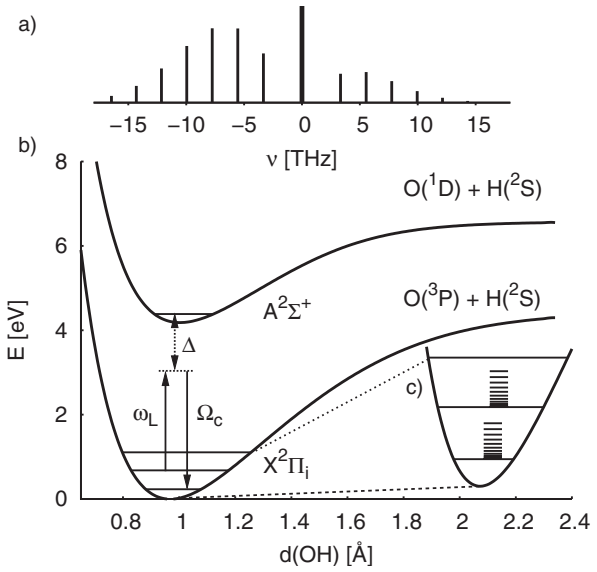

FIG. 2. (a) Simulated Raman spectra for the first nine rotational states of OH, which are relevantly occupied at room temperature. (b) Potential energy surfaces of the $X^2\Pi_i$ ground state and of the $A^2\Sigma^+$ excited state. The coherent Raman process is indicated by the arrows. (c) Rovibrational substructure.

The hyperfine splitting is neglected as angular momentum conservation for the rotational Raman transitions inhibits transitions between the hyperfine sublevels. At $T \approx 300$ K only the first 9 rotational states of OH are relevantly occupied, while only the vibrational ground state is populated. The selection rule $\Delta J = 0, \pm 2$ for the rotational transitions yields that the matrix elements of transitions between rotational states with opposite parity vanish, resulting in two separate ladders for the scattering processes with final states $|X, v = 0, J = 0, 1\rangle$ [21]. We assume that a preparation step has occurred, bringing the motional temperature to below 1 K. This could be realized with, e.g., helium-buffer-gas cooling [2], electrostatic filtering [22], or decelerator techniques [23,24]. The high-finesse optical cavity has a free-spectral range (FSR) of $15 \times 2\pi$ GHz, which can be realized with a Fabry-Perot-type cavity of length $L = 1$ cm. For simplicity we assume that the cavity only supports zeroth-order transverse modes. This actually underestimates the possibilities of scattering light into the cavity, since higher-order transverse modes can be combined in degenerate cavities, like confocal resonators. The cavity half-linewidth is set to $\kappa = 75 \times 2\pi$ kHz, and the coupling $g_{c,0\to0} = 2\pi \times 116$ kHz. This is achieved with a mode volume of 3.2×10^{-13} m^3, assuming a mode waist of $w_0 = 6$ μm, and a cavity finesse $F = 10^5$, i.e., a mirror reflectivity of 0.999 969. We also choose a laser wavelength of 532 nm, for which ample power is available as well as mirrors of the required quality. The frequency of the laser is far below that of the OH A-X rovibronic band. We assume to have single-frequency light of 10 W enhanced by a factor of 100 by a buildup cavity in a TEM_{00} mode, corresponding to a Rabi coupling $\Omega_{L,0\to0} = 2\pi \times 69$ GHz and frequency $\omega_L = \omega_0^{(A)} - \omega_0^{(X)} - \Delta$ with $\Delta \approx 2\pi \times 407$ THz. The latter value is sequentially varied during cooling, in order to drive (quasi-)resonantly the cooling transitions. In combination with the broad spectrum of cavity modes, the laser only needs to be varied over one FSR to address all anti-Stokes lines. Figure 3 displays the anti-Stokes Raman lines as a function of the frequency modulus the FSR. Addressing the Stokes lines (not drawn) can be avoided, given the small laser and cavity linewidths. In a confocal cavity, e.g., all higher-order transverse cavity modes will be degenerate with fundamental ones. In addition, our scheme is robust against a small number of coincidences between Stokes and anti-Stokes lines.

The cooling strategy is as follows. First, the external degrees of freedom are cooled to the cavity linewidth, corresponding to a final temperature $T \approx 4$ μK, by setting the Rayleigh transition quasiresonant with one cavity mode. The corresponding coefficients have been evaluated numerically, giving the rate of Rayleigh scattering for OH into the cavity $\Gamma^{\kappa}_{0\to0} \sim 1$ kHz, while the spontaneous rate $\Gamma^{\gamma}_{\xi\to\xi} \sim 0.5$–$2.5$ Hz. We verified the efficiency of cooling by solving the semiclassical equation for the mechanical energy [25]. For these parameters, starting from $T \sim 1$ K

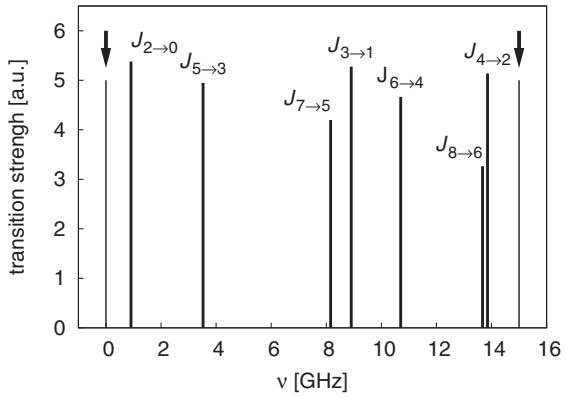

FIG. 3. Reduced spectrum of the relevant rotational anti-Stokes transitions: the lines are projected onto a single free-spectral range of the cavity, whose width is indicated by the arrows. The unfolded Raman spectrum spans 15 THz or up to 10^3 cavity modes. The frequencies of the lines are evaluated from quantum chemical calculations, and must be understood as a qualitative picture; high-resolution experimental input is needed to fix the absolute position with kHz accuracy.

for the external degrees of freedom, the cooling limit is reached in a time of the order of 1 s. Then, the rotational degrees of freedom are cooled by setting the laser frequency to sequentially address each anti-Stokes spectral line. A manually optimized sequence led to the result in Fig. 4, where the mean rotational quantum number $\langle J \rangle$ is plotted as a function of time. The final value $\langle J \rangle \approx 0.5$ corresponds to the final situation in which the two states $J = 0$ and $J = 1$, ground states of each ladder, achieve maximum occupation, equal to 50%. The insets in Fig. 4 show that after 0.3 s their occupation is about 40%, while after 1.8 s it reaches 49% (leading to a total population of 98.8%). The cooling rate for the rotational degrees of freedom of OH is of the order of 4 Hz, see Fig. 4, while the rate of heating due to spontaneous Raman scattering along the Stokes transitions is about 0.1 Hz. In the simu-

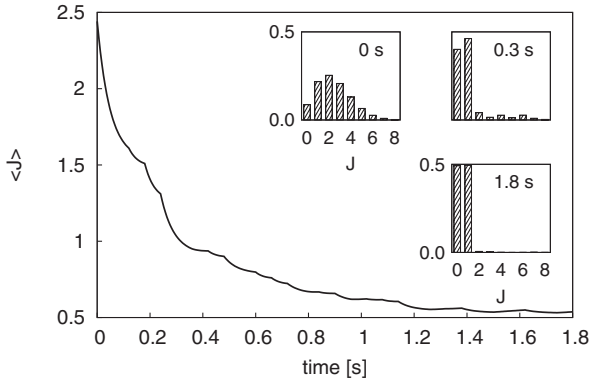

FIG. 4. Mean rotational quantum number versus time during the cooling process. The manually optimized cooling sequence first empties the levels $J = (2, 3)$, thereafter higher levels are addressed. The small figures show the state distributions at time 0, 0.3, and 1.8 s. The cavity length is fine-tuned to address the $J_{2\to0}$ and the $J_{3\to1}$ transition simultaneously.

lation the vibrational degrees of freedom are taken into account but no vibrational heating is observed. In a separate simulation, we checked that vibrational excitations are cooled with the same scheme.

The cooling time can be improved significantly for molecules with higher polarizabilities α, as the cooling rate scales with α^2. For instance, the polarizability of NO is approximately 4 times larger than for OH, and preliminary results show that it indeed cools down faster, although the cooling time is not reduced by a factor 16 because more rotational states are occupied at 300 K. For molecules like Cs_2, α is 2 orders of magnitude larger than for OH, and should yield faster cooling rates.

For molecules with low polarizability, like OH, reduction of the cooling time seems possible by further optimizing the sequential procedure. In addition, the efficiency could be improved by using degenerate cavity modes or by superradiant enhancement of light scattering, sustained by the formation of self-organized molecular crystals [26].

In summary, we presented a strategy for cooling external and internal degrees of freedom of a molecule. We simulated the cooling dynamics for OH using experimentally accessible parameter regimes, showing that this method allows for efficient preparation in the lowest rovibrational states, while the motion is cooled to the cavity linewidth. For OH the cooling time is of the order of seconds, and requires thus the support of trapping technologies which are stable over these times [2,3,27–29]. The cooling time of molecules with larger polarizabilities can scale down to a few ms, when the polarizability is about 10 times larger. Applications of this technique to polyatomic molecules has to deal with an increasing number of transitions to be addressed, which will slow down the process. A possible extension of this scheme could make use of excitation pulses, determined with optimal control techniques [7].

G. M. thanks the Theoretical Femtochemistry Group at LMU for the hospitality. Support by the European Commission (CONQUEST, No. MRTN-CT-2003-505089, EMALI, No. MRTN-CT-2006-035369), the Spanish MEC (Ramon-y-Cajal, Consolider Ingenio 2010 "QOIT", HA2005-0001), EUROQUAM (Cavity-Mediated Molecular Cooling), and the DFG cluster of excellence Munich Centre for Advanced Photonics, is acknowledged.

[1] See J. Doyle, B. Friedrich, R. V. Krems, and F. Masnou-Seeuws, Eur. Phys. J. D **31**, 149 (2004), and references therein.
[2] J. D. Weinstein, R. deCarvalho, T. Guillet, B. Friedrich, and J. M. Doyle, Nature (London) **395**, 148 (1998).
[3] M. Drewsen, A. Mortensen, R. Martinussen, P. Staanum, and J. L. Sørensen, Phys. Rev. Lett. **93**, 243201 (2004); P. Blythe, B. Roth, U. Fröhlich, H. Wenz, and S. Schiller, Phys. Rev. Lett. **95**, 183002 (2005).
[4] J. T. Bahns, W. C. Stwalley, and P. L. Gould, J. Chem. Phys. **104**, 9689 (1996).
[5] I. S. Vogelius, L. B. Madsen, and M. Drewsen, Phys. Rev. A **70**, 053412 (2004).
[6] P. W. Brumer and M. Shapiro, *Principles of Quantum Control of Molecular processes* (Wiley VCH, New York, 2003).
[7] D. J. Tannor and A. Bartana, J. Chem. Phys. A **103**, 10 359 (1999).
[8] P. Horak, G. Hechenblaikner, K. M. Gheri, H. Stecher, and H. Ritsch, Phys. Rev. Lett. **79**, 4974 (1997).
[9] V. Vuletić and S. Chu, Phys. Rev. Lett. **84**, 3787 (2000).
[10] P. Maunz, T. Puppe, I. Schuster, N. Syassen, P. W. H. Pinkse, and G. Rempe, Nature (London) **428**, 50 (2004).
[11] S. Y. T. van de Meerakker, P. H. M. Smeets, N. Vanhaecke, R. T. Jongma, and G. Meijer, Phys. Rev. Lett. **94**, 023004 (2005).
[12] J. R. Bochinski, E. R. Hudson, H. J. Lewandowski, and J. Ye, Phys. Rev. A **70**, 043410 (2004).
[13] P. Domokos and H. Ritsch, J. Opt. Soc. Am. B **20**, 1098 (2003).
[14] MOLPRO, version 2006.1, a package of *ab initio* programs, H.-J. Werner, P. J. Knowles, R. Lindh, F. R. Manby, M. Schütz, and others; see http://www.molpro.net.
[15] Convergency of the polarizability was checked by basis set enlargement. The obtained spontaneous emission rate $\Gamma = 2\pi \times 310$ kHz ($\tau = 514$ ns) for $A^2\Sigma^+$ is comparable to the value 685 ns; see J. Luque and D. R. Crosley, J. Chem. Phys. **109**, 439 (1998).
[16] J. Olsen and P. Jørgensen, J. Chem. Phys. **82**, 3235 (1985).
[17] P. Jørgensen, H. J. Aa. Jensen, and J. Olsen, J. Chem. Phys. **89**, 3654 (1988).
[18] DALTON, a molecular electronic structure program, Release 2.0 (2005); see http://www.kjemi.uio.no/software/dalton/dalton.html.
[19] K. Sundermann and R. de Vivie-Riedle, J. Chem. Phys. **110**, 1896 (1999).
[20] R. Gaufres and S. Sportouch, J. Mol. Spectrosc. **39**, 527 (1971).
[21] The anharmonicity in the vibrational ladder is included in the *ab initio* PES, the rovibrational coupling enters as $B(v)J(J+1) - D_j J^2(J+1)^2$, with $B_e = 18.871$ cm^{-1} and $\omega_e = 3735.21$ cm^{-1}; see K. P. Huber and G. Herzberg, *Molecular Spectra and Molecular Structure-IV. Constants of Diatomic Molecules* (Van Nostrand Reinhold, New York, 1979).
[22] S. A. Rangwala, T. Junglen, T. Rieger, P. W. H. Pinkse, and G. Rempe, Phys. Rev. A **67**, 043406 (2003).
[23] H. L. Bethlem, G. Berden, and G. Meijer, Phys. Rev. Lett. **83**, 1558 (1999).
[24] R. Fulton, A. I. Bishop, M. N. Shneider, and P. F. Barker, Nature Phys. **2**, 465 (2006).
[25] S. Stenholm, Rev. Mod. Phys. **58**, 699 (1986).
[26] P. Domokos and H. Ritsch, Phys. Rev. Lett. **89**, 253003 (2002); V. Vuletić, H. W. Chan, and A. T. Black, Phys. Rev. A **64**, 033405 (2001).
[27] H. L. Bethlem, G. Berden, F. M. H. Crompvoets, R. T. Jongma, A. J. A. van Roij, and G. Meijer, Nature (London) **406**, 491 (2000).
[28] D. DeMille, D. R. Glenn, and J. Petricka, Eur. Phys. J. D **31**, 375 (2004).
[29] T. Rieger, T. Junglen, S. A. Rangwala, P. W. H. Pinkse, and G. Rempe, Phys. Rev. Lett. **95**, 173002 (2005).